Effect of Oxide Presence in Activated Carbon on Arsenic Removal

Thearak Vong[1], Korea Phat[1], Seunghee Lee[1], Shinhoo Kang[1,2], and Jinhwan Oh[3,*]

[1]Department of Physics, Royal University of Phnom Penh, Phnom Penh, Cambodia
[2]Department of Materials Science and Engineering, Seoul National University, Seoul, Korea
[3]Graduate School of International Studies, Ewha Woman's University, Seoul, Korea

ARTICLE INFO

Received: 15 Mar 2023
Received in revised: 29 May 2023
Accepted: 6 Jun 2023
Published online: 4 Aug 2023
DOI: 10.32526/ennrj/21/20230066

Keywords:
Arsenic removal/ Adsorbent/ Activated carbon/ Nano oxide particles/ SDDC/ Spectrophotometry/ Cambodia

*** Corresponding author:**
E-mail: joh@ewha.ac.kr

ABSTRACT

This study investigated the effect of oxides on the removal of As when present in simple mixtures with granular activated carbon (GAC) particles. The performance of these mixtures was compared with other reported GAC-based adsorbents. A standard curve for ultraviolet adsorption vs. As concentration was obtained using the silver diethyldithiocarbamate (SDDC) method to evaluate various samples. A preliminary study was carried out to find the optimal conditions for experiments. For 50 mL samples with 2.35 ppm As, the optimal values of pH, adsorption time, and amount of adsorbent were pH 7, 30 min, and 50 mg, respectively. The ratio between the amount of adsorbent and well water in this study showed a superior As adsorption capacity (1 g/L, 2.1 mg/g) compared to similar adsorbents reported previously (12.5 g/L, 1.0-1.4 mg/g). Among the adsorbents, KOH-treated AC-Mn_3O_4 exhibited the best performance in As removal with an efficiency of ~95%. The oxide particles had a synergistic effect with GAC on As removal. This was primarily due to the change in the potential of partially agglomerated nano Mn_3O_4 particles on the ACK surface. The influence of the surface area of the adsorbents was not pronounced. All results were explained in terms of microstructure, specific surface area, and zeta potential. This finding could be extended to other activated carbons (AC) obtained from different sources.

1. INTRODUCTION

Groundwater needs to be completely protected from pollution and purified for use as a drinking water source (Gil and Vicente, 2019). Significant research efforts have been made to remove heavy metals, especially arsenic, and dye materials from water (Mahmoodi, 2014; Mahmoodi et al., 2017; Mousavi et al., 2020). Arsenic (As, hereafter) in drinking water is poisonous, mutagenic, and carcinogenic (WHO, 2010). In addition to acute poisoning, chronic exposure to modest doses of As over an extended period of time may seriously affect human health (López-Guzmán et al., 2019). In aquatic systems, inorganic As can be found in the 3^-, 0, 3^+, and 5^+ oxidation states. While the 3^+ and 5^+ oxidation states are frequently observed, the elemental states of 3^- and 0 are incredibly uncommon (Tallman and Shaikh, 1980). Inorganic As (III) and As (V) pose a potential threat to the environment, human health, and animal health. High doses of As can cause damage to the liver, skin, and central nervous, as well as cause various malignancies, including lung, skin, hyperkeratosis, and prostate cancer (Hudak, 2010; Mostafapour et al., 2013).

Although water usually contains very little As, it has a cumulative impact. Thus, numerous monitoring techniques have been developed for As, including the silver diethyldithiocarbamate (SDDC) spectrophotometric approach and novel silver salt spectrophotometry (Stratton and Whitehead, 1962; Liang and Lai, 2010; Vašák and Šedivec, 1953). The SDDC spectrophotometric approach is superior to other methods for measuring As. It is especially ideal for measuring the As concentration in large volumes of surface water and wastewater because of its excellent precision and accuracy, and cheap input costs (Liang and Lai, 2010).

Arsenic has been discovered in more than 70 nation, predominantly in Asia, but previous studies have tended to focus on Bangladesh and West Bengal (Ahmad et al., 2018). The problem in Southeast Asia,

Citation: Vong T, Phat K, Lee S, Kang S, Oh J. Effect of oxide presence in activated carbon on arsenic removal. Environ. Nat. Resour. J. 2023;21(4):345-357. (https://doi.org/10.32526/ennrj/21/20230066)

notably in Cambodia, where the highest As concentrations have been observed in the Mekong River Basin, has just been recently discovered (Pravalprukskul et al., 2018). The World Health Organization (WHO) states that the maximum allowable level of As is 10 µg/L (Yao et al., 2014). However, Cambodia maintains a much higher limit of 50 µg/L (WHO, 2011) than that of WHO.

Numerous studies have investigated the use of activated carbon (AC) for enhancing the water quality of polluted water. In addition to the As (Wong et al., 2018) cationic methylene blue dye (Jiang et al., 2021), and synthetic heavy metal ions (Pb^{2+}, Cu^{2+}, and Zn^{2+}), and Pb(II) have also been removed from an aqueous solution using AC as an adsorbent. Fe combined with Granular AC (GAC) has been used in As(V) solutions to increase the As removal efficiency (Kalaruban et al., 2019). Compared to GAC (1,013 µg/g), GAC-Fe has a greater Langmuir maximum adsorption capacity at pH 6 (1,430 µg/g) with 12.5 g/L of adsorbent in 2 h.

Another Fe-incorporated AC from a biomass combination has been fabricated via $FeSO_4$ impregnation (Rahman et al., 2020). The adsorption capacity was 42.92 mg/g. A study combining Fe_3O_4 particles with AC made from sugarcane bagasse via a chemical activation process was also reported (Joshi et al., 2019). The maximum As removal capacity of 6.69 mg/g was observed at pH 8, 1.8 g/L of adsorbent dosage, and 60 min of contact time.

Arsenic was also removed using a hybrid technique combining oxidation with ozone (Rusmana et al., 2019). Adsorption with the adsorbent doses of 12.5 g/L was 69% and 55% for GAC and zeolite, respectively. Furthermore, AC made from Tamarix leaves (Koohzad et al., 2019) showed an optimal pH of 7. With contact times of 40 min, starting concentrations of 10 mg/L, and adsorbent dosages of 3 g/L, the maximum removal efficiency was attained for As ions (96.18%). Many researchers have reported maximum As removal capacities of AC-based adsorbents that vary significantly (1-140 mg/g) (Kalaruban et al., 2019; Esmaeili et al., 2021; Jha and Maharjan, 2022). The value is presumed to be very much dependent on the manufacturing process for AC.

In this study we attempted to evaluate simple mixtures of oxide-GAC as adsorbents and compared them with other GAC-based adsorbents reported previously. Further, we made an effort to understand the effect of oxides, such as Fe_2O_3 and Mn_3O_4, in the presence of GAC on the As removal. Prior to this, an optimal condition in terms of pH, adsorption time, and amount of adsorbent was obtained. The performance was interpreted with microstructure and zeta potential.

2. METHODOLOGY

2.1 Materials and equipment

Commercial coconut GAC with a size of <2 mm was used as a raw material for As removal and purchased from Unitech Water Co., Ltd. (Cambodia). Various standard sample solutions were prepared for SDDC analysis, using a standard solution of 1,000 ppm As (Inorganic Ventures, USA). SDDC ($C_5H_{10}AgNS_2$) was procured from Shanghai Zhanyun Chemical Co., Ltd., China. A glass arsine generator was procured from Scilab Co., Ltd., Korea.

A Lamda 365 UV-VIS spectrophotometer (PerkinElmer, Korea) was used to measure the As removal efficiency. XRD (D8 Advance, Bruker, Germany) and FESEM (AUGIGA, Carl Zeiss, Germany) were employed to identify the phases and microstructures of the adsorbents, respectively. The surface area, pore size, and volume were measured using a BELSORP-MAX analyzer (Bel Japan Inc., Japan).

2.2 Preparation of adsorbents and standard curve

Iron oxide was synthesized via the copre-cipitation method, using $FeCl_3{\cdot}6H_2O$ and $FeCl_2{\cdot}4H_2O$ in DI water with 0.414 M NaOH solution. The resultant black precipitates obtained from the reaction were centrifuged, washed, and dried in an oven. For the synthesis of manganese oxide, manganese (II) nitrate tetrahydrate, $Mn(NO_3)_2{\cdot}4H_2O$, and ammonia (NH_4OH) were used (Chang and Shih, 2018). The precipitates obtained from the reaction were washed and dried in an oven. The dried manganese oxide powder was calcined in a tube furnace for 1 h at 350°C to enhance the crystallinity of the oxide precipitates (Dehmani and Abouarnadasse, 2020).

GAC powder with size of 0.8-2.0 mm was washed with 0.1 M H_2SO_4 and DI water. Then, the samples were dried at 100°C for 24 h in a dry oven. Then, KOH was mixed according to the AC:KOH weight ratio of 1:6 to improve the surface condition of GAC. The mixture was heated at 5°C/min to 750°C and cooled at 10°C/min. The resultant GAC was termed as ACK (1:6). The adsorbents were simply prepared by mixing the oxide powder with the granular ACK powder in DI water, in weight ratio of 10:1. Details of the experimental procedure are described in elsewhere (Chang and Shih, 2018; Thearak, 2023).

Various samples with known As concentrations were prepared from a standard solution of 1,000 ppm

As and DI water. Regression analysis was done to establish a standard curve of As concentration vs. UV absorbance. Then, the SDDC colorimetric technique was employed to analyze the samples treated with various adsorbents. The average values of 4-12 measurements are reported herein and the range of the variation in the values is presented with error bars.

3. RESULTS AND DISCUSSION

3.1 Characteristics and morphology of raw materials

Figure 1 shows the FESEM micrographs of as-received AC and oxides, α-Fe_2O_3 and Mn_3O_4. The as-received and as-screened AC had an irregular and granular shape with many internal pore channels, and the particle size of the as-screened AC was in the range of 0.8-2.0 mm. Iron oxide produced by co-precipitation had a diameter of 100-500 nm and was somewhat faceted. The particle size of manganese oxide differed greatly from that of iron oxide. It was in the range of 50-100 nm. Both oxides were agglomerated due to their small sizes.

In the XRD analysis of as-received AC, typical carbon peaks were observed with peak broadening (Figure 2). It indicates a low level of crystallinity of the phase. The iron and manganese oxides were identified as α-Fe_2O_3 and Mn_3O_4, respectively, with some unidentified peaks. The peak broadening is clearly reduced for the oxides, confirming the high level of crystallinity.

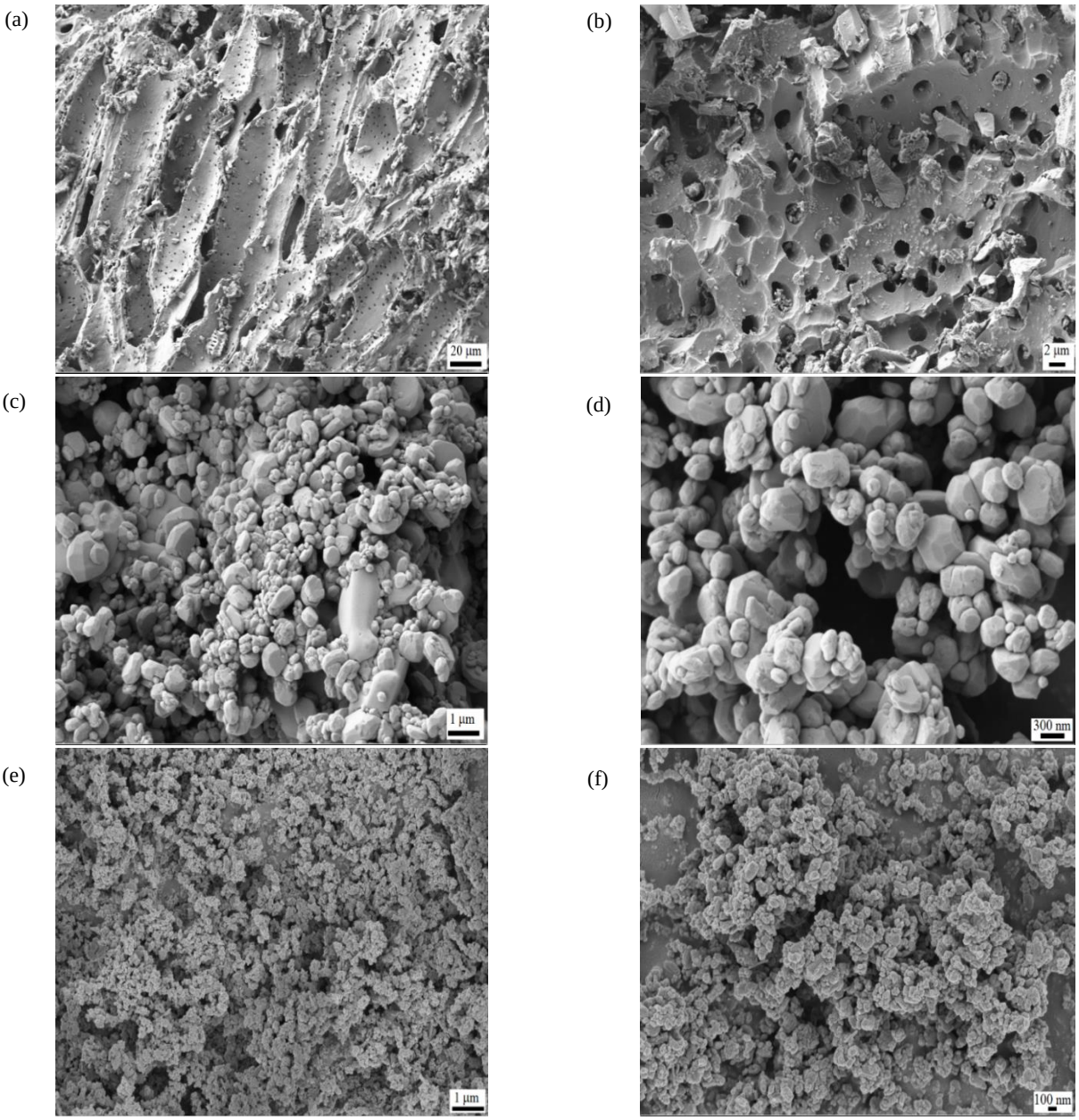

Figure 1. FE-SEM Micrographs of (a,b) As-received AC, (c,d) Fe_2O_3 and (e,f) Mn_3O_4

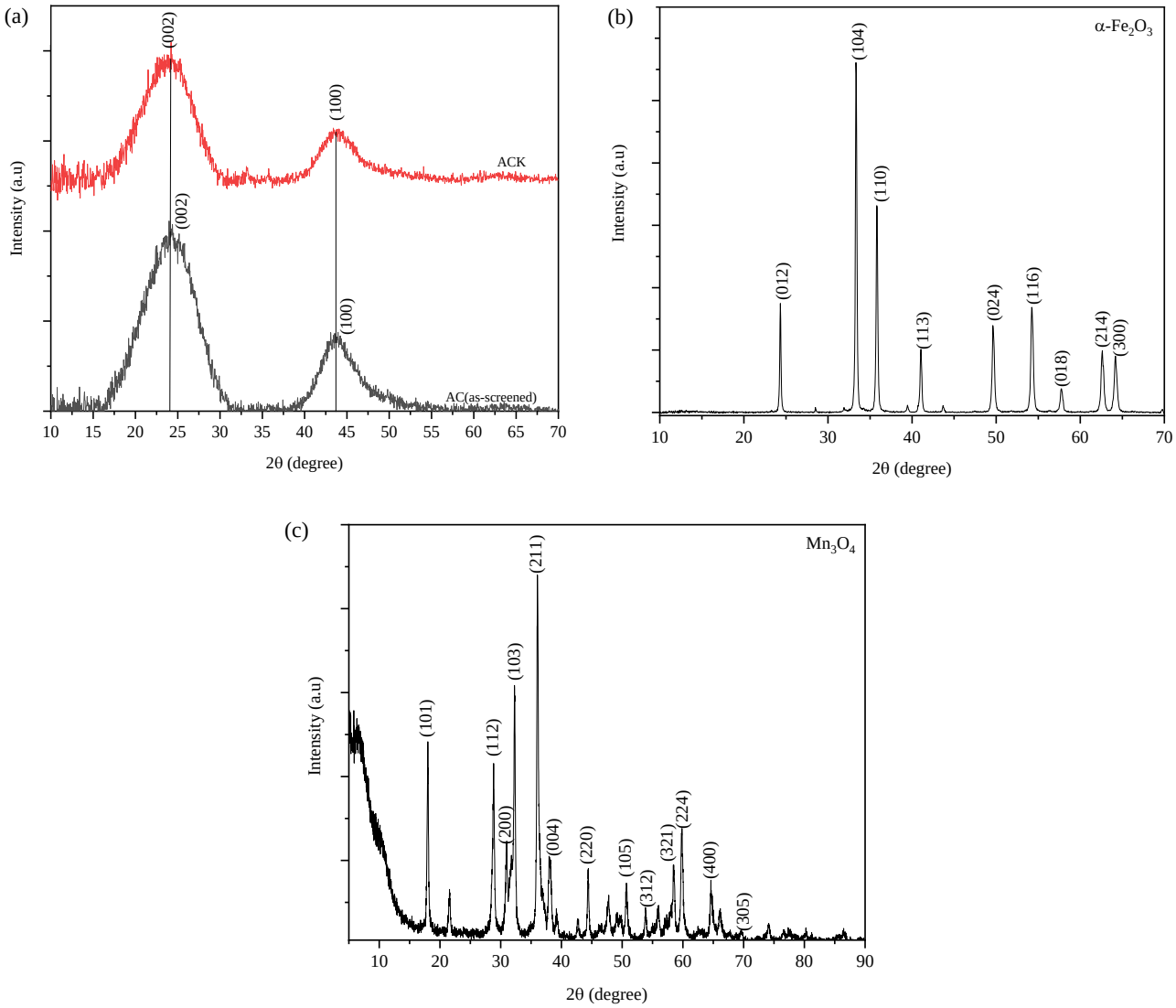

Figure 2. XRD Results from (a) AC(as-screened) and ACK, (b) α-Fe_2O_3, and (c) Mn_3O_4

Figure 3 presents the optical (a) and FESEM micrographs (b-d) of the as-screened AC and ACK (1:6). AC is commonly treated with KOH to increase the specific surface area. However, the treatment in this study did not change the surface morphology noticeably. It might be due to the large size of the employed GAC powder. But it removed most debris from the surface of the As-screened AC.

Table 1 shows the powder characteristics of the raw materials (1-4) and candidate adsorbents (5,6). The AC selected herein provides the most surface area with a high volume of nano pores. The surface area of ACK was reduced slightly compared to that of the as-screened AC. This indicates that the KOH treatment did not increase the volume of the nano pores, resulting in little increase in the surface area.

Interestingly, the BET values of both oxides were relatively small despite their nano sizes. This is attributed to the high degree of agglomeration of the powders after the co-precipitation. The powder mixture of ACK with the oxides, candidate adsorbents, showed interesting results: the BET values were considerably higher (15%~20%) than the arithmetic averages of the raw materials. Since the surface area of ACK remains constant, the increase in the area must have resulted from the oxides. That is, the oxide particles became somewhat deagglomerated during the mixing process with ACK in DI water.

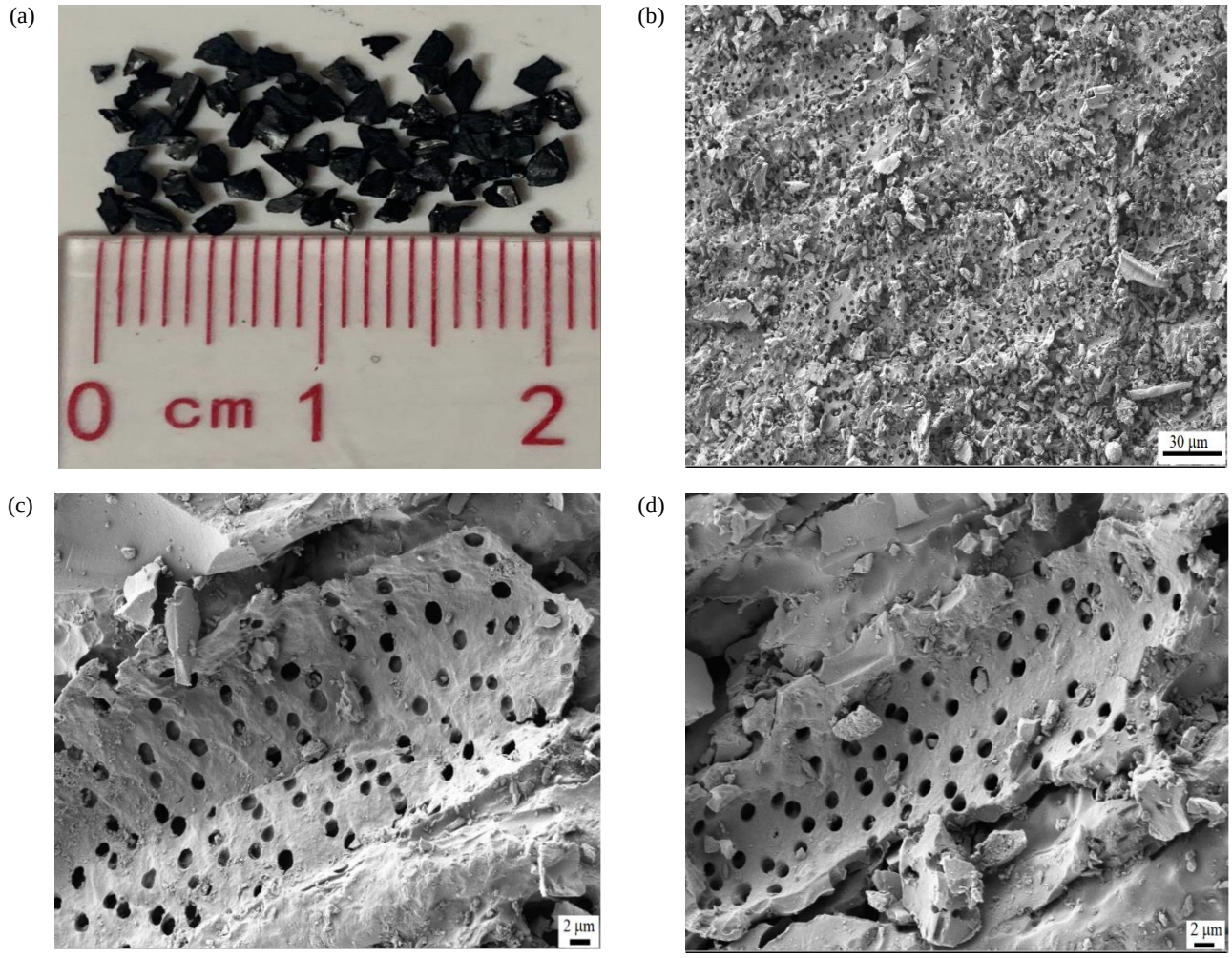

Figure 3. Microstructures of (a,b) As-screened AC and (c,d) ACK

Table 1. BET results of various AC, oxides, and their mixtures

Nº	Sample name	Surface area (m^2/g)	Total pore volume (cm^3/g)	Average pore diameter (nm)
1	AC(as-screened)	953.24	0.3855	1.6175
2	ACK (1:6)**	940.16	0.3775	1.6059
3	Fe_2O_3	2.2583	0.0011	1.9527
4	Mn_3O_4	15.463	0.1592	41.171
5	ACK-Fe_2O_3 (10:1)**	1008.10 (854.90)*	0.4086	1.6213
6	ACK-Mn_3O_4 (10:1)**	953.86 (856.10)*	0.4136	1.7342

(* Number in parentheses) Calculated BET based on the weight ratio from ** and surface area of individual sample material

3.2 Optimal conditions for As adsorption

Figure 4 is the plot of absorbance vs. As concentration obtained by SDDC method with standard samples: SDDC reacted with $AsH_{3(g)}$ that evaporated from the As-containing solution (Vašák and Šedivec, 1953). The intercept, slope of the curve, and the regression coefficient (R^2) were 0.017, 0.983, and 0.994, respectively. This demonstrates the validity of the SDDC method as it confirms the excellent linear relationship between the As concentration and As absorbance measured via spectrometry. The difference in As contents between the original solution and SDDC was calculated as the As removal amount (in %) by the adsorbent employed.

A study was conducted as a function of pH, adsorption (contact) time, and amount of adsorbent to determine the optimal and practical conditions for water purification. The sample water was obtained from a well in Kaoh Thum District, Kandal Province, Cambodia. Water was initially pumped out for five min to avoid stagnant well water. The well water of pH ~7 was immediately acidified after it was taken

from the well to pH <2 using H_2SO_4 to preserve the As concentration (Liang and Lai, 2010). The pH value of the water was adjusted later according to the experimental needs.

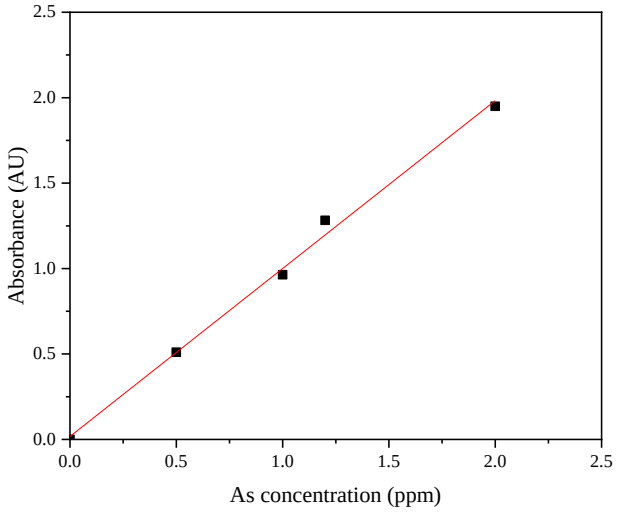

Figure 4. A plot of absorbance vs As concentration in ppm by SDDC method

Chemical analysis was done on the well water. Harmful elements such as F, B, CN, Cr, Pb, Cd, and Hg were present within the allowed limits. It was found that the As content was exceedingly high (460 µg/L) compared to the suggested WHO limit (<10 µg/L) and the Cambodian limit (<50 µg/L). For this study, the well water was condensed to a high As concentration, 2.35 ppm, by drying. Detailed results can be found in the reference (Thearak, 2023).

3.2.1 Effect of pH

The effect of pH was investigated with the candidate adsorbents. 50 mg of various adsorbents were added to 50 mL of well water, and the adsorption process was conducted for 30 min. Figure 5(a) shows the removal efficiency of the raw materials, i.e., AC, ACK (1:6), α-Fe_2O_3, and Mn_3O_4. In general, the As adsorption was not favorable in an acidic environment except for α-Fe_2O_3, as reported in previous studies (Kalaruban et al., 2019; Joshi et al., 2019).

AC (as-screened) and ACK (1:6) exhibited their best performances at pH 7, while α-Fe_2O_3 and Mn_3O_4 did at pH 5 and 9, respectively. This was expected since the ZPC of AC is normally in the pH range of 2-5 (Kalaruban et al., 2019). Further, most oxide surfaces are hydrated and result in positively and negatively charged surfaces at low and high pH values, respectively (Rahaman, 2017). ACK (1:6), which has a high surface area as presented in Table 1, exhibited ~70% As adsorption at pH 7. The performances of the two oxides were about the same.

The removal efficiency of the mixture absorbents made of the raw materials was also compared with that of ACK (Figure 5(b)). In general, a neutral water of pH 7 and/or a base water exhibited a superior performance among this limited number of samples. The highest removal of As (~95%) was observed at pH 7.0 with ACK-Mn_3O_4. Thus, pH 7.0 was chosen as the optimum condition for further experiment.

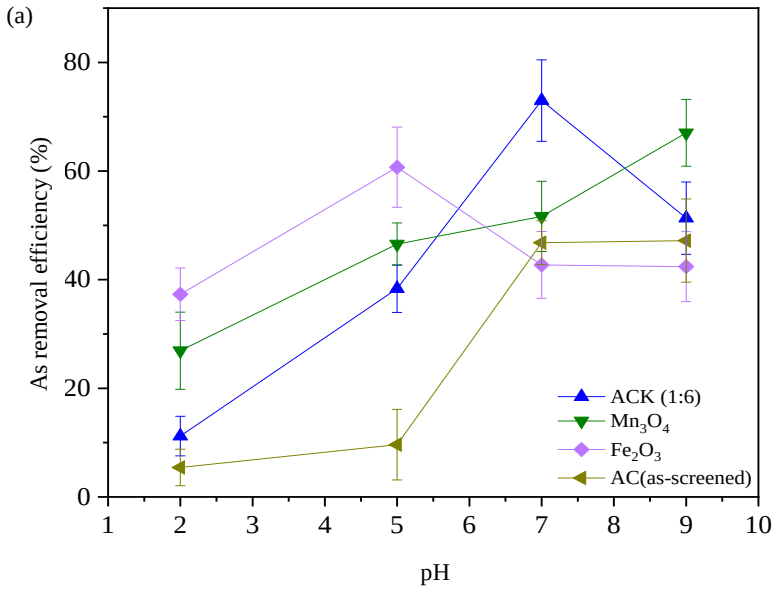

Figure 5. The effect of solution pH on Arsenic removal efficiency of (a) the raw materials and (b) the mixtures

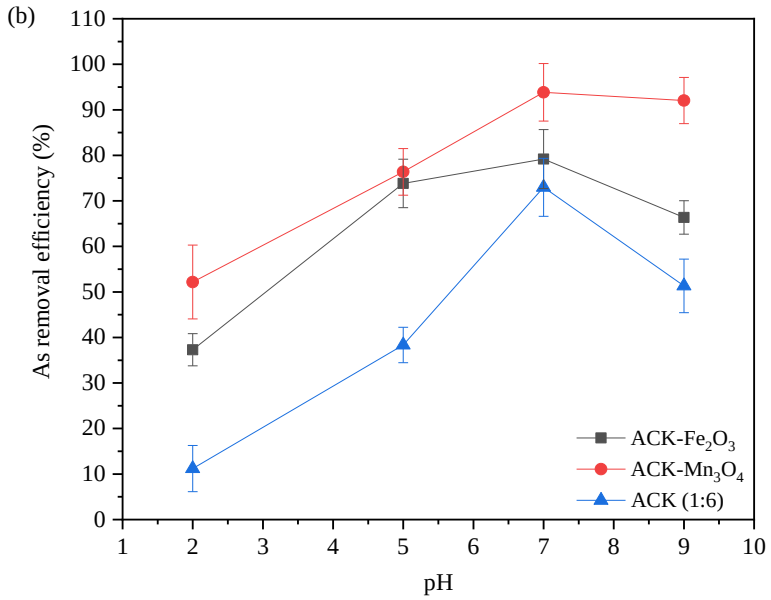

Figure 5. The effect of solution pH on Arsenic removal efficiency of (a) the raw materials and (b) the mixtures (cont.)

3.2.2 Effect of adsorption time

The removal process was conducted at pH 7 as a function of time and the amount of KOH used for AC. The maximum efficiency of 40-75% was observed within 20-60 min for various AC as shown in Figure 6(a), as was observed in previous studies (Jiang et al., 2021; Kalaruban et al., 2019; Joshi et al., 2019; Rahman et al., 2020; Rusmana et al., 2019; Koohzad et al., 2019). Considering the ratio of AC and KOH, the weight ratio of 1:6 exhibited a steady increase in the adsorption, reaching up to 70-75%. Most AC showed little improvement after 30 min. That is, the rate of removal is initially high and then stabilizes after 30 min.

A similar trend was noted from the individual oxide and candidate adsorbents (Figure 6(b)). This might be related to the intrinsic adsorption behavior that occurs on the adsorbent surface as in a Langmuir model (Tan et al., 2008). From the materials aspect, the mixtures of ACK with oxides demonstrated 75-95% efficiency in 30 min. Especially, ACK-Mn_3O_4 outperformed the others with 90-95% efficiency for the well water. Thus, a time period of 30 min was found sufficient at pH 7 for the As adsorption.

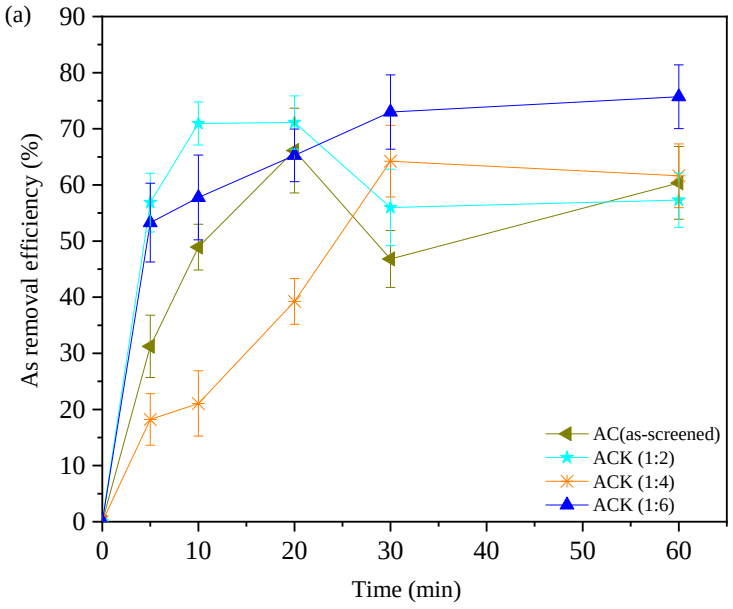

Figure 6. Arsenic removal efficiency As a function of adsorption time at pH 7 from (a) AC treated by various KOH amounts and (b) the mixtures and raw materials

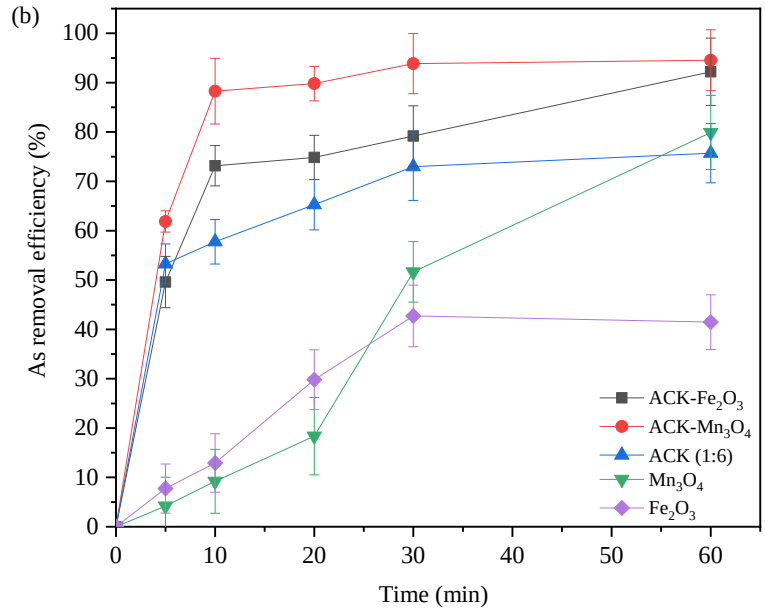

Figure 6. Arsenic removal efficiency As a function of adsorption time at pH 7 from (a) AC treated by various KOH amounts and (b) the mixtures and raw materials (cont.)

3.2.3 Effect of adsorbent amount

Figure 7 shows how various adsorbents behave, at pH 7 in 30 min of adsorption time, as a function of the adsorbent amount (10-100 mg). In most cases, the As removal rate in ppm/mg sec is high when the amount of adsorbent is relatively small (up to 50 mg). Thus, 50 mg of adsorbent was chosen for 50 ml of well water as the proper adsorption amount. In this study the as-received AC and the individual oxide showed the low rates of adsorption while the rates of ACK, ACK-Fe_2O_3, and ACK-Mn_3O_4 were high in this range (10-50 mg). It indicates that the surface morphologies of ACK, ACK-Fe_2O_3, and ACK-Mn_3O_4 offer more sites for As adsorption than those of the as-received AC and the oxides. It is to be noted that the ratio between the amount of adsorbent and well water was 1 g/L. This ratio is considerably less than the values commonly observed in other studies (1.8-12.5 g/L) (Joshi et al., 2019; Rusmana et al., 2019; Koohzad et al., 2019), demonstrating the effectiveness in practical applications and performance.

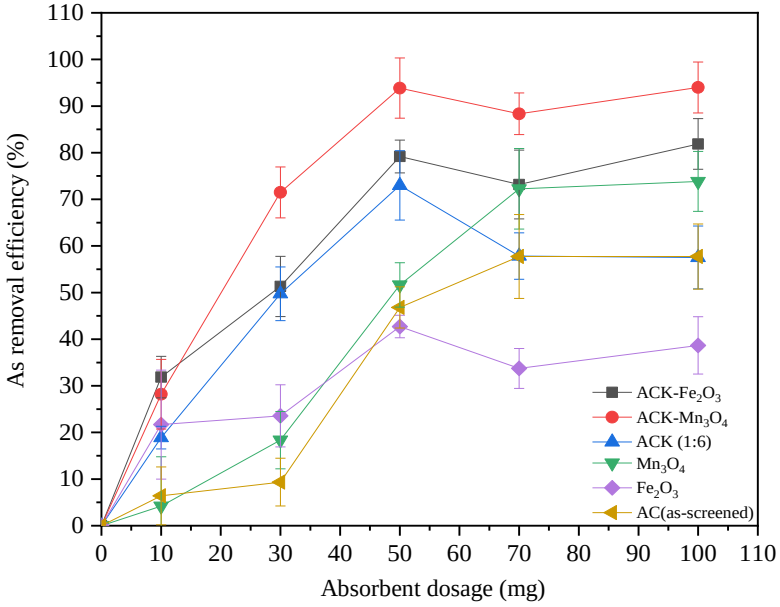

Figure 7. Arsenic removal efficiency as a function of adsorbent amount for various adsorbents at pH 7 for 30 min adsorption time

3.3 Effect of oxide presence with ACK on adsorption performance

Figure 8 presents the performance curves of ACK-Fe_2O_3 and ACK-Mn_3O_4 along with the calculated data. The dotted and dashed lines were calculated based on the weight ratio (10:1) and the surface area, respectively, of the raw materials shown in Figure 7 and Table 1. ACK-Fe_2O_3 and ACK-Mn_3O_4 performed much better than the arithmetic sums of each contribution from the constituent ACK and oxides. The simple addition of an oxide to ACK increased the As removal rate and the efficiency by 10-40% in most ranges of pH, adsorption time, and adsorbent amount. It can be concluded that the addition of oxides, especially Mn_3O_4, to ACK demonstrate a synergetic effect on the As removal.

According to Table 1, the surface areas of ACK-Fe_2O_3 and ACK-Mn_3O_4 (10:1) increased by 154 and 99 m^2/g, respectively, more than the calculated surface areas in parenthesis. As mentioned, the oxides must be responsible for the increase, which is due to deagglomeration of oxide particles. However, the addition of nano Mn_3O_4 to ACK did not result in as significant an increase in the surface area as Fe_2O_3. It means that nano Mn_3O_4 still exhibits a stronger agglomeration tendency than Fe_2O_3 due to its high surface energy associated with nano size particles.

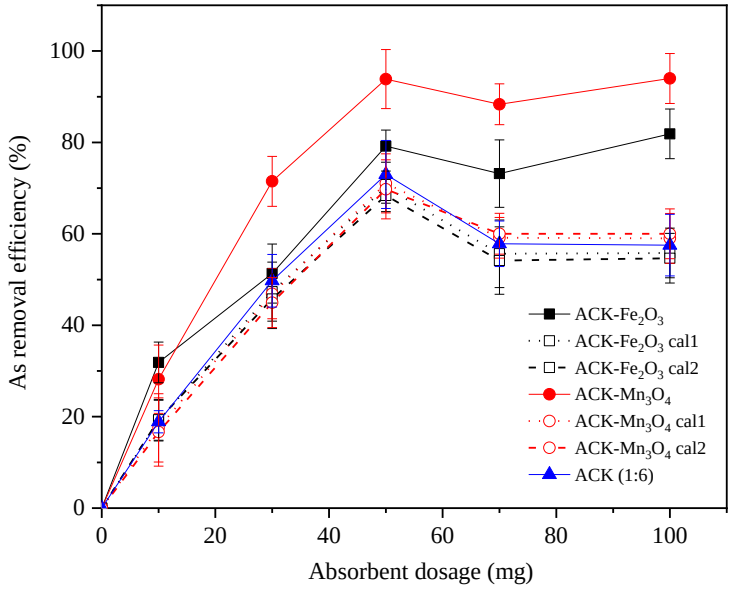

Figure 8. Effect of composition and surface area on the As removal (Calculations were done based on the weight ratio (dotted lines) and the ratio of surface areas (dashed lines) of individual constituent materials.)

Based on the results above, the colloidal states of ACK-Fe_2O_3 and ACK-Mn_3O_4 could be speculated during As adsorption. Since ACK-Fe_2O_3 exhibited a higher increase in the surface area than ACK-Mn_3O_4, Fe_2O_3 particles are expected to disperse more freely in the well water than Mn_3O_4 particles. In addition, ACK-Fe_2O_3 resulted in little improvement in the performance compared to that of ACK. Thus, it is reasonable to say that Fe_2O_3 did not enhance the number of adsorption sites for As significantly. On the other hand, Mn_3O_4 particles of nano size have a tendency to retain the state of agglomeration and deposit on the ACK surface more than Fe_2O_3 to reduce the surface energy effect. Agglomeration of powder in solid state is an equivalent term to flocculation tendency in colloidal science. Figure 9 shows the schematics of the mixture adsorbents, i.e., ACK-Fe_2O_3 and ACK-Mn_3O_4, before and after mixing the oxides with ACK in a solution.

In order to understand this issue, zeta, ζ, potential was measured for each material as a function of pH. The potential is electric, which is normally in the range of -100 to 100 mV in the interfacial double layer at the location of the slipping plane. It is normally used to estimate the dispersion tendency of particles in a solution (Dukhin and Goetz, 2017). Fast flocculation is known to occur in a solution if the potential falls in the range of 0-5 mV, while an incipient instability (low flocculation) occurs when the potential is in the range of 10-30 mV (Kumar and Dixit, 2017).

(a) ACK-Fe_2O_3

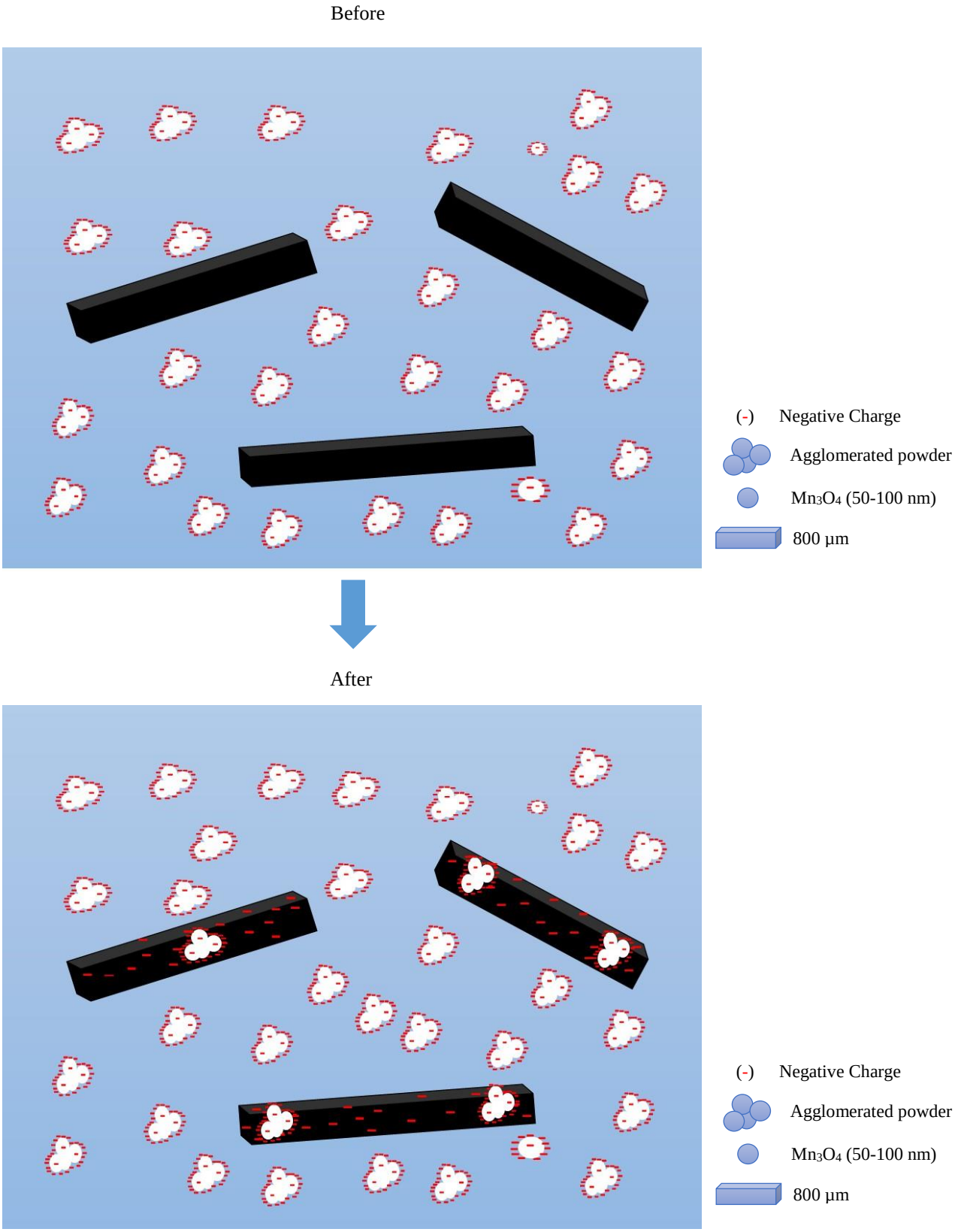

Figure 9. Schematics of (a) ACK-Fe_2O_3 and (b) ACK-Mn_3O_4 in the colloidal state before and after interactions of the mixtures

(b) ACK-Mn_3O_4

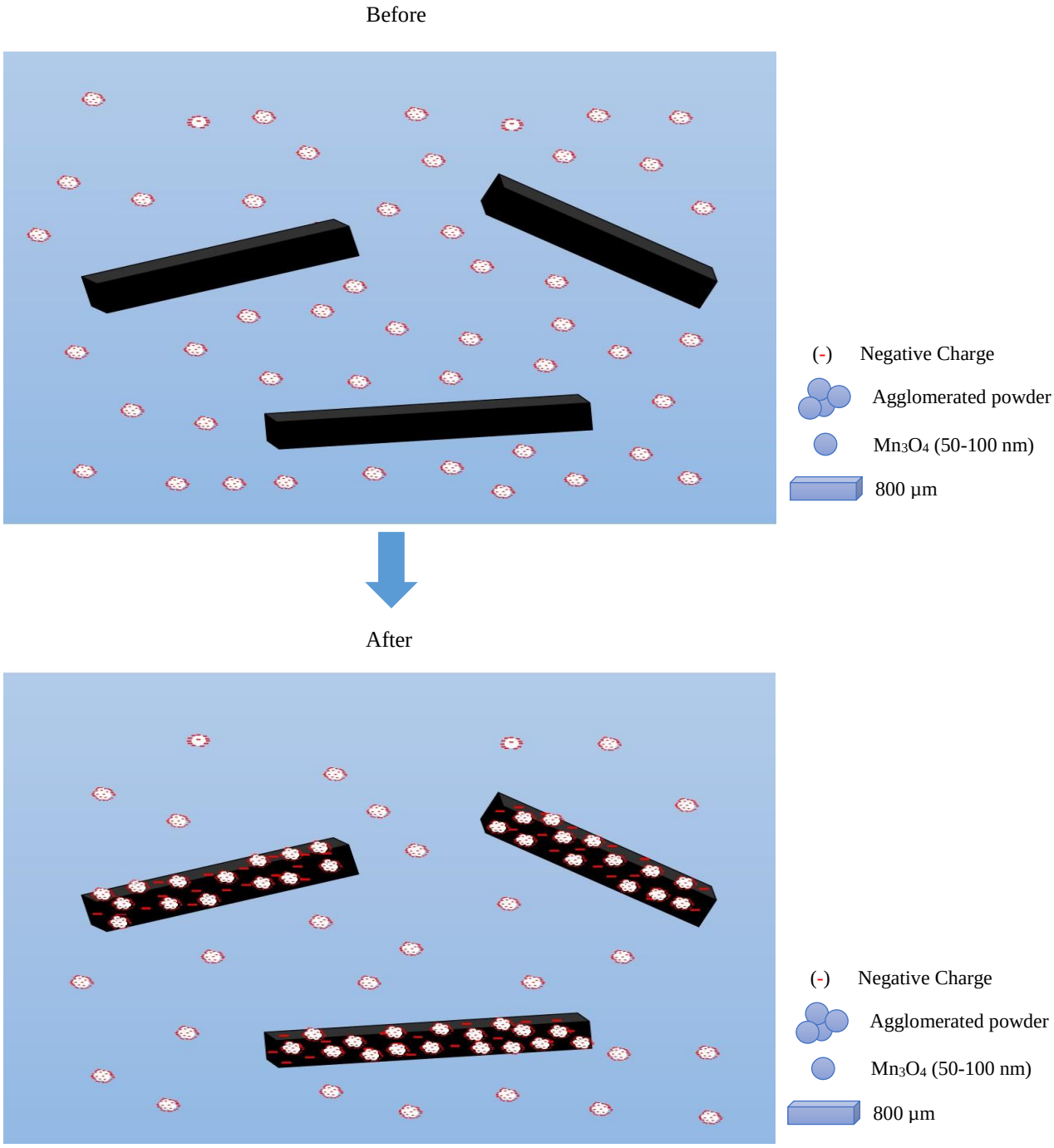

Figure 9. Schematics of (a) ACK-Fe_2O_3 and (b) ACK-Mn_3O_4 in the colloidal state before and after interactions of the mixtures (cont.)

As shown in Figure 10, the net electrical charge bounded by the slipping plane of each material ranged from 0 to -14 mV in the well water of pH 7. The zeta potential of AC and ACK was -11 mV and that of each oxide was about -12.5 mV. On the other hand, ACK-Fe_2O_3 and ACK-Mn_3O_4 had zeta potentials of -13 and -5 mV, respectively. Note that the zeta potential of ACK-Fe_2O_3 (-13 mV) is much more negative than that of ACK-Mn_3O_4 (-5 mV).

The potential of the electrical double layers is determined greatly by the surface charges of individual constituent particles, the morphology and the interactions among them. The zeta potential of ACK-Fe_2O_3 (-13 mV) is not much different from its raw materials, ACK (-11 mV), and Fe_2O_3 (-12 mV). This indicates that ACK and Fe_2O_3 particles are dispersed freely in the well water. In contrast the zeta potential of ACK-Mn_3O_4 (-5 mV) is much lower than

those of constituent materials, ACK (-11 mV) and Mn_3O_4 (-12.5 mV). It suggests that there must be intimate interactions between ACK and Mn_3O_4, providing a new environment for As adsorption.

With the known contribution of ACK in the potential, this result is in good agreement with the schematics suggested (Figure 9). The new morphology of ACK-Mn_3O_4 mixture provided the highest number of adsorption sites. A notable synergetic effect between ACK and Mn_3O_4 on As removal was observed and was reasoned by the surface charge and surface energy of the nano-sized oxide particles.

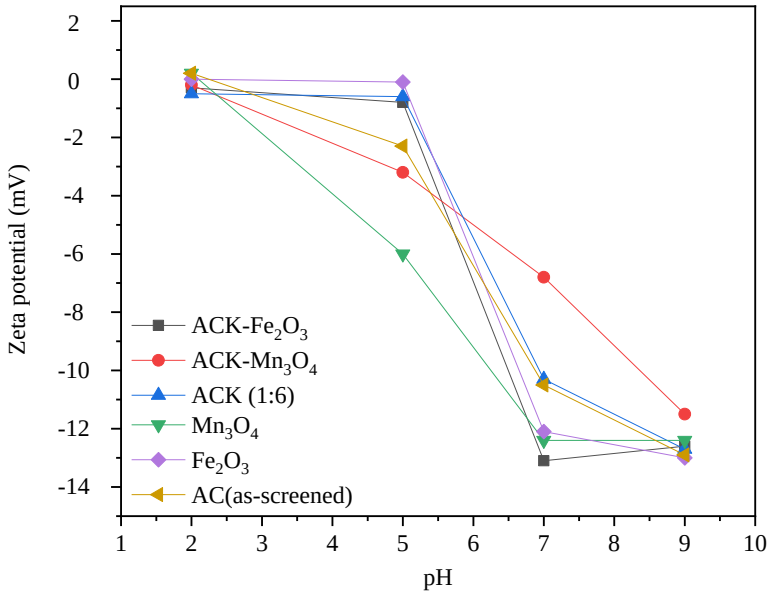

Figure 10. Zeta(ζ) potentail of various absorbents

4. CONCLUSION

The microstructure and characteristics of various AC-based adsorbents were investigated and evaluated in terms of their As removal efficiency. Overall, the study results demonstrate that adsorbents comprising ACK, Mn_3O_4, and Fe_2O_3 could be considered as economical and effective adsorbents for As removal. The summary and conclusions of this study are as follows:

(1) For 50 mL As-containing well water, the optimal values of pH, adsorption time, and amount of adsorbent were pH 7, 30 min, and 50 mg, respectively. The ratio between the amount of adsorbent and well water (1 g/L) of this study offered equivalent or superior performance efficiency compared to those reported previously (1.8-12.5 g/L). The adsorbents consisting of ACK and oxides are advantageous in performance and cost over other GAC-based adsorbents.

(2) A strong synergetic effect of Mn_3O_4 with granular ACK was observed on As removal (~95%). This is primarily due to the change in the potential of partially agglomerated nano Mn_3O_4 particles on the ACK surface. The influence of the surface area of the adsorbents was not pronounced.

Once As-removal absorbents are developed, making them widely available to public is another important task, where the role of the Cambodian government is important. Given that arsenic issues are inherently inter-disciplinary between environment and health, together with education (for raising public awareness) and coordination (between the central government and local provinces), a number of ministries (Ministry of Environment, Ministry of Health, Ministry of Rural Development, etc.) should establish systematic channels for effective communications and implementations, including communications with international communities. This should be reserved as a topic for a further study.

ACKNOWLEDGEMENTS

This work was supported by the Ministry of Education of the Republic of Korea and the National Research Foundation of Korea (NRF-2022S1 A5A2A01045555), and partially supported by the Swedish International Development Cooperation Agency (SIDA) through Sweden and Royal University of Phnom Penh (RUPP)'s Pilot Research Cooperation Program (Sida Contribution No. 11599) and We acknowledge the experimental assistance of Mr.

Piseth Lim from RUPP and Prof. GH. Lee, Dr. CH. Kim from Seoul National University.

REFERENCES

Ahmad SA, Khan MH, Haque M. Arsenic contamination in groundwater in Bangladesh: Implications and challenges for healthcare policy. Risk Management and Healthcare Policy 2018;11:251-61.

Chang M, Shih YH. Synthesis and application of magnetic iron oxide nanoparticles on the removal of Reactive Black 5: Reaction mechanism, temperature and pH effects. Journal of Environmental Management 2018;224:235-42.

Dehmani Y, Abouarnadasse S. Study of the adsorbent properties of nickel oxide for phenol depollution. Arabian Journal of Chemistry 2020;13(5):5312-25.

Dukhin AS, Goetz PJ. Characterization of Liquids, Dispersions, Emulsions, and Porous Materials Using Ultrasound. 3rd ed. Elsevier; 2017.

Esmaeili H, Mousavi SM, Hashemi SA, Chiang WH, Abnavi SA. Activated carbon@ MgO@ Fe_3O_4 as an efficient adsorbent for As (III) removal. Carbon Letters 2021;31:851-62.

Gil A, Galeano LA, Vicente MÁ. Applications of Advanced Oxidation Processes (AOPs) in Drinking Water Treatment. Cham: Springer International Publishing; 2019.

Hudak PF. Nitrate, arsenic and selenium concentrations in the pecos valley aquifer, West Texas, USA. International Journal of Environmental Research 2010;4(2):229-36.

Jha VK, Maharjan J. Activated carbon obtained from banana peels for the removal of AS (III) from water. Scientific World 2022;15(15):145-57.

Jiang W, Zhang L, Guo X, Yang M, Lu Y, Wang Y, et al. Adsorption of cationic dye from water using an iron oxide/activated carbon magnetic composites prepared from sugarcane bagasse by microwave method. Environmental Technology 2021;42(3):337-50.

Joshi S, Sharma M, Kumari A, Shrestha S, Shrestha B. Arsenic removal from water by adsorption onto iron oxide/nano-porous carbon magnetic composite. Applied Sciences 2019;9(18):Article No. 3732.

Kalaruban M, Loganathan P, Nguyen TV, Nur T, Johir MA, Nguyen TH, et al. Iron-impregnated granular activated carbon for arsenic removal: Application to practical column filters. Journal of Environmental Management 2019;239:235-43.

Koohzad E, Jafari D, Esmaeili H. Adsorption of lead and arsenic ions from aqueous solution by activated carbon prepared from tamarix leaves. ChemistrySelect 2019;4(42):12356-67.

Kumar A, Dixit CK. Methods for characterization of nanoparticles. In: Advances in Nanomedicine for the Delivery of Therapeutic Nucleic Acids. United Kingdom: Woodhead Publishing; 2017.

Liang M, Lai Y. Determination of the arsenic content in surface water by silver diethyldithiocarbamate spectrophotometry. Proceedings of the 4th International Conference on Bioinformatics and Biomedical Engineering; 2010 Jun 18-20; Chengdu: China; 2010.

López-Guzmán M, Alarcón-Herrera MT, Irigoyen-Campuzano JR, Torres-Castañón LA, Reynoso-Cuevas L. Simultaneous removal of fluoride and arsenic from well water by electrocoagulation. Science of the Total Environment 2019; 678:181-7.

Mahmoodi NM, Ghezelbash M, Shabanian M, Aryanasab F, Saeb MR. Efficient removal of cationic dyes from colored wastewaters by dithiocarbamate-functionalized graphene oxide nanosheets: From synthesis to detailed kinetics studies. Journal of the Taiwan Institute of Chemical Engineers 2017;81:239-46.

Mahmoodi NM. Synthesis of magnetic carbon nanotube and photocatalytic dye degradation ability. Environmental Monitoring and Assessment 2014;186(9):5595-604.

Mostafapour FK, Bazrafshan E, Farzadkia M, Amini S. Arsenic removal from aqueous solutions by *Salvadora persica* stem ash. Journal of Chemistry 2013;2013:Article No. 740847.

Mousavi SR, Asghari M, Mahmoodi NM. Chitosan-wrapped multiwalled carbon nanotube as filler within PEBA thin film nanocomposite (TFN) membrane to improve dye removal. Carbohydrate Polymers 2020;237:Article No. 116128.

Pravalprukskul P, Aung MT, Wichelns D. Arsenic in Rice: State of Knowledge and Perceptions in Cambodia. Stockholm: Stockholm Environment Institute; 2018.

Rahaman MN. Ceramic Processing and Sintering. Boca Raton: CRC Press; 2017.

Rahman HL, Erdem H, Sahin M, Erdem M. Iron-incorporated activated carbon synthesis from biomass mixture for enhanced arsenic adsorption. Water, Air, and Soil Pollution 2020;231:1-7.

Rusmana YF, Notodarmojo S, Helmy Q. Arsenic removal in groundwater by integrated ozonation and adsorption by activated carbon and zeolite. IOP Conference Series: Materials Science and Engineering 2019;536(1):Article No. 012073.

Stratton G, Whitehead HC. Colorimetric determination of arsenic in water with silver diethyldithiocarbamate. Journal-American Water Works Association 1962;54(7):861-4.

Tallman DE, Shaikh AU. Redox stability of inorganic arsenic (III) and arsenic (V) in aqueous solution. Analytical Chemistry 1980;52(1):196-9.

Tan IA, Ahmad AL, Hameed BH. Adsorption of basic dye on high-surface-area activated carbon prepared from coconut husk: Equilibrium, kinetic and thermodynamic studies. Journal of Hazardous Materials 2008;154(1-3):337-46.

Vašák V, Šedivec V. Colorimetric determination of arsenic. Collection of Czechoslovak Chemical Communications 1953;18(1):64-72.

Thearak V. Oxides and Activated Carbon on Removal of Arsenic from Cambodian Well Water [dissertation]. Phnom Penh, Royal University of Phnom Penh; 2023.

World Health Organization (WHO). Hardness in Drinking-Water: Background Document for Development of WHO Guidelines for Drinking-Water Quality. WHO; 2010.

World Health Organization (WHO). Guidelines for Drinking-Water Quality: WHO Chronicle. Switzerland: WHO; 2011.

Wong S, Ngadi N, Inuwa IM, Hassan O. Recent advances in applications of activated carbon from biowaste for wastewater treatment: A short review. Journal of Cleaner Production 2018;175:361-75.

Yao S, Liu Z, Shi Z. Arsenic removal from aqueous solutions by adsorption onto iron oxide/activated carbon magnetic composite. Journal of Environmental Health Science and Engineering 2014;12:1-8.